

1 **Title:** ~~Basin-scale connections between reach-scale sediment respiration and~~ Point-scale organic-matter
2 decomposition in streambeds is weakly associated with reach-scale respiration

3
4 James C. Stegen^{1,2*}, Morgan Barnes¹, Dillman Delgado¹, Brieanne Forbes¹, Vanessa A. Garayburu-
5 Caruso¹, Amy E. Goldman¹, Maggi Laan^{1,3}, Sophia McKeever¹, Peter Regier¹, Lupita Renteria¹, Scott D.
6 Tiegs⁴

7 *Correspondence: James.Stegen@pnnl.gov

8 1. Pacific Northwest National Laboratory, Richland, WA, United States

9 2. Washington State University, Pullman, WA, United States

10 3. University of California, Riverside, CA, United States

11 4. Oakland University, Rochester, MI, United States

12
13 **Abstract**

14 Stream and river ecosystems play a central role in the movement and decomposition of particulate
15 organic matter, serving as a conduit between terrestrial hillslopes and coastal environments.

16 ~~Microbial~~Microbe-catalyzed decomposition generates simpler organic molecules that fuel respiration,
17 often in the sediments of these ecosystems. However, the degree of connection between sediment-
18 associated respiration (ER_{sed}) and organic-matter decomposition potential remains poorly understood.

19 ~~How that relationship compares to decomposition's relationship~~ It is also unclear whether organic-
20 matter-decomposition potential is more closely associated with ER_{sed} , whole-ecosystem respiration
21 ~~(ER_{tot}) and), or water-column respiration (ER_{wc})~~ respiration is also not clear. We examined the link
22 between particulate organic-matter decomposition potential—using cellulose-based cotton strips as a
23 standardized substrate—and all three components of respiration across 48 sites in the environmentally
24 diverse Yakima River Basin (Washington State, USA). We hypothesized that decomposition within
25 sediments would be most strongly related to ER_{sed} , but decomposition rates were more closely
26 associated with ER_{tot} , less so with ~~little connection to~~ ER_{sed} ~~or~~ and not at all with ER_{wc} . This suggests that
27 point-scale particulate organic-matter decomposition potential within stream/river sediments ~~reflects~~
28 more closely associated with integrated system respiration rather than with processes confined to
29 sediments or the water column alone though these relationships were weak overall. Further, across the
30 basin, decomposition rates nearly spanned the previously reported global range for streams and rivers
31 and were best explained by total dissolved nitrogen (TDN), sediment grain size, and aridity of the
32 upstream drainage area. These results highlight the strong influence of land cover and basin-scale
33 biophysical variation on sediment-associated decomposition processes and indicate that mechanistic
34 models of organic-matter decomposition in streams ~~and~~ rivers should account for coupled sediment-
35 water-land interactions.

36 **Key words:** Yakima River; organic-matter decomposition; sediment respiration; stream metabolism;
37 cotton-strip assay; hyporheic zone respiration

38

39

40 **Introduction**

41 Stream networks are major components of the global carbon cycle (Cole et al., 2007; Drake et al., 2018;
42 Talluto et al., 2024). Whole-stream metabolism is often studied as an integrated outcome of processes
43 occurring across the continuum from the air-water interface down through sediments that are below
44 the stream itself (Battin et al., 2023; Tank et al., 2010). The sediments include the interface between the
45 streambed and water column (i.e., the benthic zone) and the spatial domain below this interface,
46 referred to as the hyporheic zone (Boulton et al., 1998; Krause et al., 2011; Wondzell, 2011). The benthic
47 zone can be highly productive with significant primary producer (e.g., algae) and heterotrophic microbial
48 biomass (Allan et al., 2021). The hyporheic zone is also highly biogeochemically active due, in part, to
49 surface water flowing through it and mixing with groundwater to stimulate heterotrophic microbial
50 activity (Boano et al., 2014; Lewandowski et al., 2019; Zarnetske et al., 2011). Processes occurring on
51 and around sediments across the benthic-to-hyporheic continuum are often jointly responsible for the
52 bulk of biogeochemical activity in stream systems (Burrows et al., 2017; Fellows et al., 2001; Garayburu-
53 Caruso et al., 2025; Naegeli and Uehlinger, 1997), with important exceptions in large rivers (Roley et al.,
54 2023).

55 Metabolic processes within integrated stream systems are linked to the building of and breaking down
56 of organic matter (Hall and Hotchkiss, 2017a; Odum, 1956). Streams are commonly net heterotrophic
57 ~~whereby~~, meaning they ~~release~~ ~~mineralize~~ more ~~organic-matter-associated~~ carbon than they
58 ~~accumulate~~ ~~fix by in-stream primary production~~ (Battin et al., 2023; Bernhardt et al., 2022). This
59 emphasizes the importance of understanding organic-matter decomposition in streams and its
60 connection to respiration rates, which are ultimately linked to rates of elemental cycling. Organic-matter
61 decomposition is commonly measured in stream systems by quantifying the breakdown of specific
62 substrates (Benfield et al., 2017; Woodward et al., 2012). Cellulose-based cotton strips are an
63 increasingly common model substrate for such studies as they enable broad comparisons across streams
64 (and other types of ecosystems)(Colas et al., 2019; Filbee-Dexter et al., 2022; Tiegs et al., 2024; Vyšná et
65 al., 2014). ~~Like other standardized substrates used in decomposition studies (e.g., litter bags), cotton-~~
66 ~~strips quantify organic-matter-decomposition potential, that is, the capacity of the ecosystem to~~
67 ~~decompose organic matter, rather than the actual rate of native organic-matter decomposition *in situ*.~~ A
68 standard approach is to place them in the field for a known amount of time, retrieve them, and measure
69 the loss in tensile strength, as a ~~proxy for~~ ~~measure of~~ the degree of decomposition. This approach has
70 revealed many factors that impact decomposition in streams such as temperature, land use, aqueous
71 chemistry, sediment texture, stream flow, location within the stream network, and canopy cover,
72 among others (Griffiths and Tiegs, 2016; Tiegs et al., 2024).

73 ~~Previous~~ Studies have examined the relationship between organic_matter decomposition and whole-
74 stream respiration (Mancuso et al., 2023; Pingram et al., 2020; Young and Collier, 2009), but have not
75 specifically tied organic_matter decomposition within sediments to sediment-associated respiration. This
76 leads to an open question and the focus of our study: To what degree are point-scale rates of organic-
77 matter_decomposition ~~potential~~ within sediments linked to reach-scale respiration associated with the
78 whole-stream ecosystem (ER_{tot}), the sediments (ER_{sed}), or the water column (ER_{wc})? ER_{tot} represents
79 reach_scale aerobic respiration from autotrophs and heterotrophs across benthic, planktonic, and
80 hyporheic zones. ER_{sed} comprises reach_scale sediment-associated respiration from benthic ~~and~~

81 streambed sediments, rooted ~~and~~ submerged plants, and hyporheic zones that are hydrologically
82 connected to the active channel, ~~and~~; ER_{wc} constitutes reach-scale planktonic respiration occurring only
83 in the water column.

84 We specifically tested the hypothesis that reach-scale ER_{sed} rates are strongly linked to point-scale
85 measurements of organic-matter decomposition within streambed sediments. More specifically, we
86 tested the prediction that cotton-strip-decay rates ~~will be~~ best explained by ER_{sed} , with little
87 additional variation in decay rates explained by ER_{tot} or ER_{wc} . To test our hypothesis and associated
88 prediction we used field deployments across the Yakima River Basin (YRB). The YRB is an
89 environmentally diverse basin in southeastern Washington State (USA) that is $\sim 16,000$ km² and with a
90 stream network that culminates in the 7th-order Yakima River. To generate the data needed to test our
91 hypothesis, we used a combination of sensors and cotton strips across 48 sites in the YRB that
92 collectively spanned a continuum from small mountainous streams in coniferous forests with little
93 human impact to a large lowland river in an arid environment surrounded by significant agricultural land
94 use. The resulting patterns help to fill a fundamental knowledge gap in our understanding of how point-
95 scale organic-matter-decomposition potential relates to reach-scale respiration and can be used to
96 inform models that aim to mechanistically integrate biogeochemical processes within and across stream
97 networks.

98

99 **Methods**

100 To evaluate the linkages between organic-matter decomposition and stream ecosystem respiration we
101 took advantage of a prior study (Garayburu-Caruso et al., 2025) that separated ER_{tot} , ER_{sed} , and ER_{wc}
102 across environmentally divergent locations in the YRB (Fig. 1). Garayburu-Caruso et al. (2025) used
103 dissolved oxygen (DO) sensors, dark bottle incubations, and the single-station method (Odum, 1956) to
104 estimate these three components of respiration. In addition, that study deployed sensors to log water
105 temperature, used here to calculate cumulative degree days, as described below. These and associated
106 contextual data were downloaded from existing data packages (Delgado et al., 2023; Forbes et al., 2023;
107 Garayburu-Caruso et al., 2023), and methods are described in detail by Garayburu-Caruso et al. (2025).
108 In brief, DO timeseries were analyzed via StreamMetabolizer (Appling et al., 2018) to estimate ER_{tot} . The
109 length of the reach that a given DO sensor integrates varies across streams and has been
110 estimated to be roughly three times the turnover length of O₂ (Hall and Hotchkiss, 2017b). As such,
111 integrated reach lengths likely varied across sites due to differences in reaeration and discharge.
112 Field sites were located in separate, non-overlapping reaches, helping to minimize potential spatial
113 autocorrelation between neighboring sites in the estimated metabolic rates. To estimate ER_{wc} , 2 L
114 opaque bottles containing a DO sensor were filled with stream water and incubated *in situ*; the rate of
115 DO drawdown was used as the estimate of ER_{wc} . The difference between ER_{tot} and ER_{wc} was used as an
116 estimate of ER_{sed} , which represents all respiration in the stream system that is not directly occurring in
117 the water column. ER_{sed} therefore includes respiration in the hyporheic zone, the streambed surface,
118 and rooted/submerged plants. We note, however, that ER estimates derived from open diel O₂ methods
119 capture all oxygen-consuming processes, not solely aerobic respiration. These estimates could also
120 include abiotic oxidation of dissolved Fe(II) or the oxidation of other end products from anaerobic
121 metabolism (Demars et al., 2015; Piatka et al., 2021), other oxidation processes such as nitrification and
122 photooxidation of organic matter (Demars et al., 2015; Estapa and Mayer, 2010), or O₂ inputs from
123 groundwater (Hall and Tank, 2005). Because ER_{sed} was calculated by the difference between ER_{tot} and
124 ER_{wc} , it may be sensitive to these non-respiratory O₂ sinks. However, biological metabolism is generally

125 [considered the dominant O₂-consuming pathway in streams and we therefore interpret ER_{sed} primarily](#)
126 [as sediment-associated biological O₂ consumption while acknowledging that other contributions may be](#)
127 [captured.](#)

128 To take advantage of the ecosystem respiration study, cotton strips made of Artist fabric (following the
129 protocol of Tiegs et al., 2013) were deployed at the same time as the DO sensors. They were deployed
130 upstream of the DO sensors to capture the upstream reach that influenced the DO sensor readings and
131 prevent disturbance during sensor maintenance. [This design prioritized among-reach coverage across](#)
132 [the basin \(48 sites\) and provided point-scale estimates of decomposition potential at a single location](#)
133 [within each reach.](#)

134 The cotton strips were deployed ~~at~~in the ~~interface between water and sediments~~[shallow hyporheic zone](#)
135 for 35 continuous days at 48 sites across the YRB (Fig. ~~1~~[1](#)). [At each site, deployment locations were](#)
136 [selected to be representative of the reach in terms of sediment size, flow velocity, and substrate](#)
137 [composition. In larger river systems \(e.g., 7th-order reaches\), deployments were limited to wadeable](#)
138 [areas near channel margins.](#) Deployment and retrieval days varied across four days, but all strips were
139 deployed for 35 days: deployments were from July 25th to July 28th, 2022 and retrievals were from
140 August 29th to September 1st, 2022. Cotton strips were cut from bolts of 12-ounce, heavy-weight cotton
141 fabric composed of 95% cellulose (Style 548; Fredrix, Lawrenceville, GA, USA). Each strip was 27 threads
142 wide and cut to 8.0 cm by 2.5 cm. [\(after Tiegs et al. 2013\).](#) Each cotton strip was laid flat in a stainless-
143 steel mesh cage (10.8 x 4.5 cm, RSV Jumbo Mesh Herb Infuser) to minimize physical damage and feeding
144 by macroinvertebrates, thereby emphasizing microbe-based decomposition. At each site, four cages
145 with one strip each were attached to the underside of clay bricks (20 x 10 x 5.5 cm) with stainless steel
146 wire. The brick/cage/strip setup was nestled into streambed sediment such that the cages/strips were
147 within the sediments and the brick was at the sediment/water interface. The four cages were next to
148 each other. This setup kept the cotton strips out of direct light and within the sediments while allowing
149 water to flow past the cotton strips.

150 After the 35-day incubation period, cotton strips were carefully removed from cages and gently brushed
151 with gloved hands in stream water for approximately 10 s to remove large debris. Cleaned cotton strips
152 were placed in 50 mL conical centrifuge tubes with 70% ethanol. Tubes were capped and rolled
153 approximately 10 times before ethanol was removed, ~~and~~. [After completing this step,](#) clean 70% ethanol
154 was added to the 50 mL tube to minimize further microbial-based decomposition. Cotton strips were
155 transported in the ethanol filled tubes on blue ice to Pacific Northwest National Laboratory in Richland,
156 WA. At the laboratory, the ethanol was removed from the tubes and cotton strips were air dried
157 overnight prior to further drying in an oven at 40 °C for at least 24 hours. After drying, cotton strips were
158 stored in air-tight containers with desiccant.

159 Dried cotton strips were shipped to Oakland University, [Rochester, MI](#) for tensile-strength analysis
160 following the protocol in Tiegs et al., (2013). A tensiometer was used to estimate tensile strength (Mark
161 10 MG100 with a Chatillon TCM 201 with roller jaws). The tensiometer pulled each cotton strip at a rate
162 of 2 cm/min. Some of the cotton strips were completely degraded such that there was no material to
163 measure, while other cages only contained fragments that were too small to measure tensile strength.
164 [These non-detect strips accounted for 5.4% of all deployed strips.](#) In both cases, a limit of detection was
165 assigned as the lowest tensile strength calculated in Tiegs et al. (2019) divided by 2, resulting in a final
166 value of 0.05. This was done to avoid statistical artifacts that can arise when simply introducing a value

167 of 0- (i.e., the natural log transformation in Equation 1 would be undefined). Removing these strips
168 entirely would bias the analyses away from conditions with very fast decomposition.

169 Tensiometer data were converted into decay rates using tensile loss calculated via Equation 1 (as in
170 Mancuso et al., 2022).

$$171 \quad K = \frac{-\ln(T_s/T_{sc})}{Time} \quad \text{Equation 1}$$

172 Here, K is the decomposition rate, T_s is the post-incubation tensile strength of the deployed cotton
173 strips, and T_{sc} is the mean tensile strength of control strips that were not incubated in the field. The time
174 variable was calculated as either the number of chronological deployment days (i.e., 35 days) or the
175 number of degree days. Using degree days as the time variable accounts for variation in temperature
176 across field sites and was estimated separately for each site as the sum of mean daily river temperature
177 over the incubation period. We use K_{cd} and K_{dd} to represent decay rate per chronological day or per
178 degree day, respectively. The values of K_{cd} and K_{dd} were estimated for each individual cotton strip and
179 then replicates were averaged to provide a single site-level value for K_{cd} and K_{dd} .

180 We examined both K_{cd} and K_{dd} to evaluate whether the connection between decomposition and reach-
181 scale respiration rates depends on accounting for temperature variation across the study basin. This is
182 particularly relevant in the YRB because our field sites ranged from colder headwater streams to warmer
183 low-gradient rivers. To test our hypothesis, we conducted both univariate and multivariate regression-
184 based analyses. We used ordinary least squares regression to examine the strength of univariate
185 correlations between K_{cd} or K_{dd} and ER_{tot} , ER_{wc} , or ER_{sed} . We complemented this univariate analysis with
186 multiple regression analysis to find an optimized model to explain variation in either K_{cd} or K_{dd} .

187 Further, to explore how other system variables may explain further variation in decomposition rates, a
188 LASSO (Least Absolute Shrinkage and Selection Operator) regression model was built using physical,
189 chemical and environmental variables (Table S1) as inputs, and K_{cd} or K_{dd} as the response variables.
190 Variables were cube root transformed and z-score normalized to reduce the impact of high leverage
191 points in the regression analysis and to equally weight all variables. The LASSO regression was
192 performed over 100 iterations, each with a different random seed using the `cv.glmnet` function in the
193 `glmnet` R package (Friedman et al., 2010). β coefficients were normalized to the maximum β coefficient
194 for each iteration, then averaged over the 100 iterations for the final reported value. Both the raw and
195 normalized mean β coefficient and standard deviation are reported in addition to the R^2 (Table 2).

196

197 **Results and Discussion**

198 **Decomposition in the Yakima River Basin spans globally reported rates**

199 Both K_{cd} and K_{dd} exhibited a wide range of values (Fig. 2), effectively spanning the theoretical maximum
200 of what could have been observed with our deployment setup. This is evidenced by some cotton strips
201 being completely consumed prior to retrieval (5.4% of all strips, K_{cd} and K_{dd} maximized), while others
202 were largely intact (K_{cd} and $K_{dd} \approx 0$). This variation is surprising given the relatively small spatial domain
203 sampled by this study, and emphasizes that environmental heterogeneity can surpass the effects of
204 spatial extent (Mancuso et al., 2022). The environments studied here ranged from pristine locations in
205 the mountainous headwaters of the YRB to lowland locations with heavy agricultural influences (Fig. 1;

206 Laan et al. 2025). This emphasizes the value of [climatically](#)[environmentally](#) diverse watersheds like the
207 YRB as useful testbeds to study variation in decomposition rates within single hydrologically connected
208 basins.

209 Comparing decay rates from the YRB to a global dataset from > 500 streams and rivers (Tiegs et al.,
210 2024) showed that YRB rates spanned nearly the entire global range and had substantial overlap with
211 the bulk of the global distributions (Fig. 2a,b). Dominant peaks in the YRB rate distributions were shifted
212 slightly towards faster rates, relative to primary peaks in the global dataset (Fig. 2a,b). This shift towards
213 faster rates and the wide range in rates ~~may be because YRB are likely due to several factors linked to~~
214 rates ~~were being~~ estimated in later summer, ~~a time of year when decay processes are likely maximized~~
215 ~~due to relatively~~ [with](#) high temperatures, and ~~slow flows~~ [established biological communities due to](#)
216 [several months since high-flow disturbances](#) (Collier et al., 2013b; Grimm and Fisher, 1989; Mancuso et
217 al., 2023). The two decay rates were also closely correlated with each other, though the relationship
218 weakened towards locations with faster decay rates (**Fig. 2c**). This suggests a weak influence of
219 temperature in the YRB; a strong influence of temperature should lead to a weak relationship between
220 K_{cd} and K_{dd} . These results ~~are surprising given~~ [contrast](#) previously reported influences of temperature on
221 particulate organic-matter decomposition (Benbi et al., 2014; Griffiths and Tiegs, 2016), ~~and likely~~
222 [reflect dominance of other influential factors such as variation in nutrient concentrations \(Rosemond et](#)
223 [al. 2015\)](#). Temperature-driven decomposition is also expected to lead to a strong relationship between
224 K_{cd} and summed temperature, but we observed a very weak relationship despite ~4-fold variation in
225 summed temperature (**Fig. 2d**). This range in temperature among sites would likely be smaller in other
226 seasons, and we do not therefore expect a strong influence of temperature to emerge in the YRB by
227 conducting the study in other seasons. These results emphasize the need to understand factors
228 governing variation in decay rates across the YRB. This is especially true given that rate distributions
229 within this one basin span nearly all globally observed decay rates.

230 Across the YRB there appears to be potential for some spatial organization for both K_{cd} and K_{dd} (**Fig. 3**).
231 Visual inspection of the maps suggests that the spatial organization may be stronger for K_{cd} than for K_{dd} .
232 To evaluate this possibility more rigorously, we regressed each decay rate against upstream drainage
233 area (Fig. 4). In this case, drainage area is meant to reflect position within the YRB. We used drainage
234 area in preference to stream order because it is a continuous variable directly tied to the spatial domain
235 a given stream integrates, whereas stream order is categorical and primarily reflects stream network
236 topology. Associated regressions were significant ($p < 0.05$) with both decay rates increasing with
237 drainage area (**Fig. 4**). The relationship with drainage area was stronger, in terms of R^2 , for K_{cd} . Both
238 relationships were, however, relatively weak with R^2 values of 0.22 and 0.14 for K_{cd} and K_{dd} , respectively
239 (**Fig. 4**). Nonetheless, the existence of a significant relationship after controlling for temperature (i.e., for
240 K_{dd}) indicates that spatially structured factors other than temperature influence decay rates. This is not
241 surprising as studies using cotton strips have found several factors that influence decomposition, such as
242 nutrient concentrations, turbidity, and many others (Collier et al., 2013b; Pingram et al., 2020; Tiegs et
243 al., 2024). Before exploring a broad suite of potential explanatory variables, we tested our hypothesis
244 that decomposition rates will be better explained by sediment-associated respiration (ER_{sed}) than by
245 respiration in the water column (ER_{wc}) or by respiration of the integrated stream system (ER_{tot}).

246

247 **Respiration in sediments explains little variation in decomposition**

248 Contrary to our hypothesis, we found that both decay rates were most strongly connected to ER_{tot} , less
249 so with ER_{sed} , and not at all with ER_{wc} (**Fig. 5**). Univariate models using ER_{tot} were better than multivariate
250 models using ER_{sed} , ER_{wc} , and their interaction. This is evidenced by univariate models using ER_{tot} having
251 AIC values more than two units lower than multivariate models containing ER_{sed} and ER_{wc} (**Table 1**).
252 Multivariate models were not used with ER_{tot} because it contains ER_{sed} and ER_{wc} . [Garayburu-Caruso et](#)
253 [al., 2025 showed that \$ER_{sed}\$ accounted for the majority of \$ER_{tot}\$ across most of the YRB, with 88% of](#)
254 [locations showing \$ER_{sed}\$ contributions exceeding 50% of \$ER_{tot}\$. The strong correspondence between these](#)
255 [two metrics might explain the similar \$R^2\$ values observed. We note, however, that the difference in](#)
256 [explained variance between \$ER_{tot}\$ \(\$R^2 = 0.29\$ for \$K_{cd}\$; \$R^2 = 0.16\$ for \$K_{dd}\$ \) and \$ER_{sed}\$ \(\$R^2 = 0.22\$ for \$K_{cd}\$; \$R^2 = 0.13\$](#)
257 [for \$K_{dd}\$ \) was modest, and the stronger association with \$ER_{tot}\$ should be interpreted cautiously.](#)

258 ~~To interpret these results are surprising, in part, because the~~, we note that cotton strips were deployed
259 ~~within the shallow hyporheic zones (i.e., within a few centimeters into the riverbed sediments), beneath~~
260 ~~a brick set flush with the streambed surface. We conceptualized this deployment strategy is a key as the~~
261 ~~shallow hyporheic zone, which was a~~ reason we hypothesized that decay rates would be most strongly
262 connected to ER_{sed} . However, the results indicate that [point-scale](#) decomposition of particulate organic
263 matter within the shallow hyporheic zone is linked to respiratory processes occurring in both the
264 sediment and water column. [Therefore, our deployment depth might have reflected sediment-water](#)
265 [interface processes in addition to shallow hyporheic zone processes, leading to stronger associations of](#)
266 [cotton strip decomposition with \$ER_{tot}\$. We also note that \$ER_{sed}\$ estimates may not exclusively reflect](#)
267 [biological respiration, as non-respiratory \$O_2\$ -consuming processes can contribute to these estimates \(see](#)
268 [Methods\).](#) We propose that if our deployment configuration was complemented with a simultaneous
269 deployment that enabled growth of benthic algal biofilms on the cotton strips, the combined
270 decomposition from both deployments ~~would~~[could, in some systems](#), capture ~~substantially~~ more of the
271 processes that contribute to ER_{sed} . This would provide a more complete view of sediment-associated
272 biogeochemical function, potentially leading to a stronger correlation between decomposition rates and
273 ER_{sed} . While this remains to be tested, the underlying idea is that primary producers support a large
274 portion of ~~heterotrophic~~ respiration associated with riverbed sediments, which is supported by recent
275 analyses showing a strong link between ER_{sed} and gross primary production across the YRB (Garayburu-
276 Caruso et al., 2025).

277 **Slower rates of K_{cd} and K_{dd} are in streams with coarse sediments, set within wet forests**

278 Given that our hypothesis was rejected and that ER_{tot} explained only about 29% and 16% of K_{cd} and K_{dd} ,
279 respectively (**Table 1, Figure 5**), we used a discovery-based approach to explore other system variables
280 that may explain further variation in decomposition rates. LASSO-based modeling indicated that total
281 dissolved nitrogen (TDN) and the median grain size of sediment texture (D50) were most important for
282 explaining K_{dd} , while TDN and aridity were most important for explaining K_{cd} (**Table 2**). Other variables
283 were retained in the LASSO models (**Table S1**), but we interpreted TDN, D50, and aridity as the most
284 important because they consistently had the largest normalized coefficients. This interpretation is based
285 on these variables having mean normalized coefficients above 0.5—in terms of absolute value—
286 meaning they were at least 50% as important as the most important variable in the 100 LASSO model
287 runs. Further, the LASSO coefficients for these variables had a coefficient of variation less than 0.5,
288 meaning that across the 100 LASSO model runs the values of their normalized coefficients were
289 relatively stable (**Table S1**). The LASSO modeling also confirmed a relatively weak influence of

290 temperature, evidenced by relatively small and highly variable β coefficients for summed temperature in
291 the K_{cd} model (Table S1); temperature was not used in the K_{dd} model.

292 Both decomposition rates increased with higher TDN concentrations, while K_{dd} decreased with larger
293 D50 and K_{cd} decreased with higher aridity index values (Table 1). To more deeply interpret these
294 relationships, we examined Pearson-based univariate correlations between these three explanatory
295 variables and other variables included in the LASSO models. This is important because of strong
296 collinearity among some explanatory variables (Fig. S1). In this case, variables identified as being the
297 most important may be acting as proxies for one or more additional variables. We found that TDN was
298 most strongly correlated with percent agricultural land cover of the upstream drainage area and sulfate
299 concentrations in the stream water (Fig. S1). Increases in both decomposition rates with TDN may,
300 therefore, reflect agricultural inputs of nutrients that increase overall microbial activity of the stream
301 ecosystems we studied. D50 was most strongly correlated with the aridity index, which was most
302 strongly correlated with percent forest cover; the correlation between D50 and aridity is unlikely to
303 reflect a causal connection, while aridity and forest cover most likely are causally linked. If the
304 relationship between decomposition and D50 is causal, it could be mediated by the total surface area
305 available for microbial attachment. [This would, however, influence decomposition only to the extent
306 that microbial biomass in adjacent sediments impacts microbial activity on the cotton strips.](#) Coarser
307 sediments have much less surface area, potentially limiting overall microbial activity.

308 Considering the directionality of the univariate relationships, in context of the LASSO outcomes,
309 suggests slower decomposition—for both rates—in streams with relatively coarse sediments and set
310 within relatively wet forests. This contrasts with Clapcott and Barmuta (2010) who found faster
311 decomposition in coarser sediments. The discrepancy is likely because we excluded macroinvertebrates
312 while they did not, and they interpreted the link to sediment texture as due to greater habitat
313 availability for macroinvertebrates in coarser sediments. Locations with slower decomposition should,
314 thus, primarily be in higher elevation, relatively pristine parts of the YRB, while faster decomposition
315 occurs at lower elevations impacted by agricultural inputs. These results are consistent with previous
316 work showing greater cotton strip decomposition in impaired streams (Young and Collier, 2009), those
317 with little natural land cover (Collier et al., 2013a; Webb et al., 2019), and in streams with higher
318 nutrient concentrations (Ferreira et al., 2015; Pingram et al., 2020; Tiegs et al., 2013). In addition to
319 differences in nutrient concentrations between higher and lower elevation sites, we expect less light
320 penetration to streams in higher elevation sites because of more forest cover and smaller streams.
321 Though not measured here, less light could suppress autotrophic production which ~~will~~ may limit
322 heterotrophic respiration (Bernhardt et al., 2022; Mulholland et al., 2001; Young and Huryn, 1999) ~~and,~~
323 ~~in turn, indirectly lead to slower decomposition.~~ [Lower autotrophic production could therefore slow
324 decomposition relative to high-light conditions by reducing the supply of labile carbon from phototrophs
325 that can prime organic-matter degradation \(Danger et al. 2013; Howard-Parker et al. 2020\).](#)

326 **Point-scale decomposition is ~~linked to~~ associated with processes across the sediment-water continuum
327 and land features**

328 Our results collectively indicate that to study shallow hyporheic zone decomposition processes, it is not
329 sufficient to conceptualize organic-matter decomposition by only considering sediment or water column
330 processes; one must examine the integrated system. The implication of our analyses is that [point-scale
331 organic_matter decomposition ~~rates are linked to the~~ potential was more closely associated with](#)

332 integrated system ~~more strongly~~ respiration than ~~they are linked to~~ with individual respiration
333 ~~components or direct interactions between components of.~~ Our findings suggest that ~~integrated system.~~
334 mechanistic models of stream ecosystem respiration, ~~therefore, need to account~~ may benefit from
335 accounting for sediment processes, water-column processes, and land-cover influences from beyond the
336 stream. Focusing exclusively on the hyporheic zone is insufficient, even in systems for which the
337 hyporheic zone accounts for most reactions (Boano et al., 2014; Burrows et al., 2017; McClain et al.,
338 2003). This is further emphasized by previous work showing that most respiration occurs in the water
339 column of large rivers (Gardner and Doyle, 2018; Roley et al., 2023). Garayburu-Caruso et al. (2025) also
340 show that fractional contributions of ER_{sed} to ER_{tot} is often high, but that there is significant variation in
341 those fractional influences across the YRB. This variability is due to ER_{wc} being fast enough, in some
342 locations, to account for more than 80% of ER_{tot} (Garayburu-Caruso et al., 2025). Similarly, Laan et al.
343 (2025) found substantial overlap between the distribution of ER_{wc} rates from the YRB and ER_{tot} from
344 across the contiguous United States. The overall picture is that decomposition is the result of integrated
345 processes occurring across the sediment-water continuum and influenced by external factors tied to
346 land cover and land use. We infer that these integrated processes are influenced by biophysical variation
347 across the YRB (Laan et al., 2025), leading to decomposition rates within this single basin that resemble
348 global rate distributions and nearly span the global range of observed rates (Tiegs et al., 2024). Other
349 basins that contain only one ecoregion or have homogeneous land cover may be expected to have a
350 ~~narrow~~ narrower range of decomposition rates (Webb et al., 2019). We note that our decomposition
351 estimates represent point-scale conditions at wadeable locations and should be interpreted as such
352 rather than as reach-integrated measures of decomposition. Capturing within-reach spatial variability in
353 decomposition across habitats and channel depths would complement the among-reach approach used
354 here, and may lead to stronger relationships between decomposition rates and reach-scale ER.
355 Nonetheless, models applied to any stream network that aim to predict spatiotemporal variation in
356 decomposition rates would be well served by considering processes throughout the integrated
357 watershed system.

358 **Code and data availability**

359 Data and scripts used to generate the main findings within this manuscript can be found at
360 <https://github.com/river-corridors-sfa/rcsfa-ST-2B-SSS-cotton-strip>. Upon acceptance of this
361 manuscript, they will be published on the U.S. Department of Energy's Environmental System Science
362 Data Infrastructure for a Virtual Ecosystem (ESS-DIVE) repository. Other data collected during the field
363 efforts (i.e., sensor data; surface water chemistry data; and geospatial information, metadata, and maps
364 for 2021 Spatial Study sampling event) can be accessed on ESS-DIVE at [https://data.ess-](https://data.ess-dive.lbl.gov/datasets/doi:10.15485/1987520)
365 [dive.lbl.gov/datasets/doi:10.15485/1987520](https://data.ess-dive.lbl.gov/datasets/doi:10.15485/1987520) (Garayburu-Caruso et al., 2023), [dive.lbl.gov/datasets/doi:10.15485/1969566](https://data.ess-
366 <a href=) (Delgado et al., 2023), and [dive.lbl.gov/datasets/doi:10.15485/1923689](https://data.ess-
367 <a href=) (Forbes et al., 2023).

368 **Author contributions**

369 Conceptualization: JCS, MB, VAGC, PR, ST

370 Data Curation: MB, JCS, BF, ML, SM, DD, LR and AEG

371 Formal Analysis: MB, MML, BF, and JCS

372 Funding Acquisition: JCS
373 Investigation: MB, DD, BF, VAGC, AEG, ML, SM. PR, LR, ST and JCS
374 Methodology: MB, DD, BF, VAGC, AEG, ML, SM. PR, LR, ST and JCS
375 Project Administration: MB, VAGC and JCS
376 Resources: MB, DD, BF, VAGC, AEG, ML, SM. PR, LR, ST and JCS
377 Software: MB, MML, BF, and JCS
378 Supervision: MB, VAGC and JCS
379 Validation: MB and JCS
380 Visualization: MB, MML, BF, and JCS
381 Writing – Original Draft Preparation: MB, VAGC, ST and JCS
382 Writing – Review & Editing: MB, DD, BF, VAGC, AEG, ML, SM. PR, LR, ST and JCS

383 **Competing interest**

384 The authors declare that they have no conflict of interest.

385 **Acknowledgements**

386 This work was supported by the River Corridor Science Focus Area (RC-SFA) at the Pacific Northwest
387 National Laboratory (PNNL). The RC-SFA is supported by the United States Department of Energy, Office
388 of Biological and Environmental Research (BER), Environmental System Science (ESS) Program. PNNL is
389 operated by Battelle Memorial Institute for the United States Department of Energy under contract no.
390 DE-AC05-76RL01830. We thank the United States Forest Service, Washington Department of Natural
391 Resources, Washington Department of Fish and Wildlife, Confederated Tribes and Bands of the Yakama
392 Nation, and Cowiche Canyon Conservancy for access to field locations where these samples were
393 collected. We also thank the Confederated Tribes and Bands of the Yakama Nation Tribal Council and
394 Yakama Nation Fisheries for working with us to facilitate sample collection and optimization of data
395 usage according to their values and worldview. We thank the field team including: Dillman Delgado,
396 Morgan Barnes, Brandon T. Boehnke, Yunxiang Chen, Kali Cornwell, Brianna I. Gonzalez, Samantha
397 Grieger, Glenn E. Hammond, Peishi Jiang, Bing Li, Zhi Li, Xinming Lin, Sophia A. McKeever, Maruti K.
398 Mudunuru, Katherine A. Muller, Opal Otenburg, Aaron Pelly, Kelsey Peta, Alan Roebuck, Joshua M.
399 Torgeson, and Jianqiu Zheng.

400

401 **References**

402 Allan, J. D., Castillo, M. M., and Capps, K. A.: Stream Ecology: Structure and Function of Running Waters,
403 Springer International Publishing, Cham, <https://doi.org/10.1007/978-3-030-61286-3>, 2021.

404 Appling, A. P., Hall Jr., R. O., Yackulic, C. B., and Arroita, M.: Overcoming Equifinality: Leveraging Long
405 Time Series for Stream Metabolism Estimation, *Journal of Geophysical Research: Biogeosciences*, 123,
406 624–645, <https://doi.org/10.1002/2017JG004140>, 2018.

407 Battin, T. J., Lauerwald, R., Bernhardt, E. S., Bertuzzo, E., Gener, L. G., Hall, R. O., Hotchkiss, E. R.,
408 Maavara, T., Pavelsky, T. M., Ran, L., Raymond, P., Rosentreter, J. A., and Regnier, P.: River ecosystem
409 metabolism and carbon biogeochemistry in a changing world, *Nature*, 613, 449–459,
410 <https://doi.org/10.1038/s41586-022-05500-8>, 2023.

411 Benbi, D. K., Boparai, A. K., and Brar, K.: Decomposition of particulate organic matter is more sensitive to
412 temperature than the mineral associated organic matter, *Soil Biology and Biochemistry*, 70, 183–192,
413 <https://doi.org/10.1016/j.soilbio.2013.12.032>, 2014.

414 Benfield, E. F., Fritz, K. M., and Tiegs, S. D.: Chapter 27 - Leaf-Litter Breakdown, in: *Methods in Stream
415 Ecology (Third Edition)*, edited by: Lamberti, G. A. and Hauer, F. R., Academic Press, 71–82,
416 <https://doi.org/10.1016/B978-0-12-813047-6.00005-X>, 2017.

417 Bernhardt, E. S., Savoy, P., Vlah, M. J., Appling, A. P., Koenig, L. E., Hall, R. O., Arroita, M., Blaszcak, J. R.,
418 Carter, A. M., Cohen, M., Harvey, J. W., Heffernan, J. B., Helton, A. M., Hosen, J. D., Kirk, L., McDowell,
419 W. H., Stanley, E. H., Yackulic, C. B., and Grimm, N. B.: Light and flow regimes regulate the metabolism of
420 rivers, *Proceedings of the National Academy of Sciences*, 119, e2121976119,
421 <https://doi.org/10.1073/pnas.2121976119>, 2022.

422 Boano, F., Harvey, J. W., Marion, A., Packman, A. I., Revelli, R., Ridolfi, L., and Wörman, A.: Hyporheic
423 flow and transport processes: Mechanisms, models, and biogeochemical implications, *Reviews of
424 Geophysics*, 52, 603–679, <https://doi.org/10.1002/2012RG000417>, 2014.

425 Boulton, A. J., Findlay, S., Marmonier, P., Stanley, E. H., and Valett, H. M.: The functional significance of
426 the hyporheic zone in streams and rivers, *Annual Review of Ecology, Evolution, and Systematics*, 29, 59–
427 81, <https://doi.org/10.1146/annurev.ecolsys.29.1.59>, 1998.

428 Burrows, R. M., Rutledge, H., Bond, N. R., Eberhard, S. M., Auhl, A., Andersen, M. S., Valdez, D. G., and
429 Kennard, M. J.: High rates of organic carbon processing in the hyporheic zone of intermittent streams,
430 *Sci Rep*, 7, 13198, <https://doi.org/10.1038/s41598-017-12957-5>, 2017.

431 Clapcott, J. E. and Barmuta, L. A.: Metabolic patch dynamics in small headwater streams: exploring
432 spatial and temporal variability in benthic processes, *Freshwater Biology*, 55, 806–824,
433 <https://doi.org/10.1111/j.1365-2427.2009.02324.x>, 2010.

434 Colas, F., Woodward, G., Burdon, F. J., Guérol, F., Chauvet, E., Cornut, J., Cébron, A., Clivot, H., Danger,
435 M., Danner, M. C., Pagnout, C., and Tiegs, S. D.: Towards a simple global-standard bioassay for a key
436 ecosystem process: organic-matter decomposition using cotton strips, *Ecological Indicators*, 106,
437 105466, <https://doi.org/10.1016/j.ecolind.2019.105466>, 2019.

438 Cole, J. J., Prairie, Y. T., Caraco, N. F., McDowell, W. H., Tranvik, L. J., Striegl, R. G., Duarte, C. M.,
439 Kortelainen, P., Downing, J. A., Middelburg, J. J., and Melack, J.: Plumbing the Global Carbon Cycle:
440 Integrating Inland Waters into the Terrestrial Carbon Budget, *Ecosystems*, 10, 172–185,
441 <https://doi.org/10.1007/s10021-006-9013-8>, 2007.

442 Collier, K. J., Clapcott, J. E., Hamer, M. P., and Young, R. G.: Extent estimates and land cover relationships
443 for functional indicators in non-wadeable rivers, *Ecological Indicators*, 34, 53–59,
444 <https://doi.org/10.1016/j.ecolind.2013.04.010>, 2013a.

445 Collier, K. J., Clapcott, J. E., Duggan, I. C., Hamilton, D. P., Hamer, M., and Young, R. G.: Spatial Variation
446 of Structural and Functional Indicators in a Large New Zealand River, *River Research and Applications*,
447 29, 1277–1290, <https://doi.org/10.1002/rra.2609>, 2013b.

448 Delgado, D., Barnes, M., Boehnke, B. T., Chen, X., Chen, Y., Cornwell, K., Forbes, B., Fulton, S. G.,
449 Garayburu-Caruso, V. A., Goldman, A. E., Gonzalez, B. I., Grieger, S., Hammond, G. E., Jiang, P., Kaufman,
450 M. H., Laan, M., Li, B., Li, Z., Lin, X., McKeever, S. A., Mudunuru, M. K., Muller, K. A., Myers-Pigg, A.,
451 Otenburg, O., Pelly, A., Peta, K., Powers-McCormack, B., Regier, P., Renteria, L., Roebuck, A., Scheibe, T.
452 D., Son, K., Torgeson, J. M., Zheng, J., and Stegen, J. C.: Spatial Study 2022: Surface Water Samples,
453 Cotton Strip Degradation, and Hydrologic Sensor Data across the Yakima River Basin, Washington, USA
454 (v3), 2023.

455 Demars, B. O. L., Thompson, J., and Manson, J. R.: Stream metabolism and the open diel oxygen method:
456 Principles, practice, and perspectives, *Limnology and Oceanography: Methods*, 13, 356–374,
457 <https://doi.org/10.1002/lom3.10030>, 2015.

458 Drake, T. W., Raymond, P. A., and Spencer, R. G. M.: Terrestrial carbon inputs to inland waters: A current
459 synthesis of estimates and uncertainty, *Limnology and Oceanography Letters*, 3, 132–142,
460 <https://doi.org/10.1002/lo.10055>, 2018.

461 Estapa, M. L. and Mayer, L. M.: Photooxidation of particulate organic matter, carbon/oxygen
462 stoichiometry, and related photoreactions, *Marine Chemistry*, 122, 138–147,
463 <https://doi.org/10.1016/j.marchem.2010.06.003>, 2010.

464 Fellows, C. S., Valett, M. H., and Dahm, C. N.: Whole stream metabolism in two montane streams:
465 Contribution of the hyporheic zone, *Limnology and Oceanography*, 46, 523–531,
466 <https://doi.org/10.4319/lo.2001.46.3.0523>, 2001.

467 Ferreira, V., Castagnyrol, B., Koricheva, J., Gulis, V., Chauvet, E., and Graça, M. A. S.: A meta-analysis of
468 the effects of nutrient enrichment on litter decomposition in streams, *Biological Reviews*, 90, 669–688,
469 <https://doi.org/10.1111/brv.12125>, 2015.

470 Filbee-Dexter, K., Feehan, C. J., Smale, D. A., Krumhansl, K. A., Augustine, S., Bettignies, F. de, Burrows,
471 M. T., Byrnes, J. E. K., Campbell, J., Davoult, D., Dunton, K. H., Franco, J. N., Garrido, I., Grace, S. P.,
472 Hancke, K., Johnson, L. E., Konar, B., Moore, P. J., Norderhaug, K. M., O’Dell, A., Pedersen, M. F.,
473 Salomon, A. K., Sousa-Pinto, I., Tiegs, S., Yiu, D., and Wernberg, T.: Kelp carbon sink potential decreases
474 with warming due to accelerating decomposition, *PLOS Biology*, 20, e3001702,
475 <https://doi.org/10.1371/journal.pbio.3001702>, 2022.

476 Forbes, B., Barnes, M., Boehnke, B. T., Bowden, M. E., Chen, X., Cornwell, K., Crawford, M., Delgado, D.,
477 Fulton, S. G., Garayburu-Caruso, V. A., Gary, S., Goldman, A. E., Gonzalez, B. I., Grieger, S., Hammond, G.
478 E., Jiang, P., Kaufman, M. H., Laan, M., Li, B., Li, Z., McKeever, S. A., Mudunuru, M. K., Muller, K. A., Myers-
479 Pigg, A., Ocejo, J. A., Otenburg, O., Pelly, A., Peta, K., Powers-McCormack, B., Regier, P., Renteria, L.,
480 Roebuck, A., Scheibe, T. D., Son, K., Tffaily, M. M., Torgeson, J. M., Stegen, J. C., and Consortium, T. W.:
481 WHONDORS River Corridor Sediment and Water Geochemistry and In Situ Sensor Data from Machine-
482 Learning-Informed Sites across the Contiguous United States (v6), 2023.

483 Friedman, J., Hastie, T., and Tibshirani, R.: Regularization Paths for Generalized Linear Models via
484 Coordinate Descent, *Journal of Statistical Software*, 33, 1–22, <https://doi.org/10.18637/jss.v033.i01>,
485 2010.

486 Garayburu-Caruso, V. A., Kaufman, M. H., Delgado, D., Barnes, M., Boehnke, B. T., Chen, X., Cornwell, K.,
487 Forbes, B., Fulton, S. G., Goldman, A. E., Gonzalez, B. I., Grieger, S., Jr, R. O. H., Hammond, G. E., Jiang, P.,
488 Laan, M., Li, B., Li, Z., Lin, X., McKeever, S. A., Mudunuru, M. K., Muller, K. A., Myers-Pigg, A., Otenburg,
489 O., Pelly, A., Peta, K., Regier, P., Renteria, L., Roebuck, A., Scheibe, T. D., Son, K., Torgeson, J. M., and
490 Stegen, J. C.: Spatial Study 2022: Water Column, Sediment, and Total Ecosystem Respiration Rates across
491 the Yakima River Basin, Washington, USA (v2), 2023.

492 Garayburu-Caruso, V. A., Kaufman, M., Forbes, B., Hall, R. O., Laan, M., Chen, X., Lin, X., Fulton, S.,
493 Renteria, L., Fang, Y., Son, K., and Stegen, J. C.: Sediment-associated processes account for most of the
494 spatial variation in ecosystem respiration in the Yakima River basin, *bioRxiv*, 2024.03.22.586339,
495 <https://doi.org/10.1101/2024.03.22.586339>, 2025.

496 Gardner, J. R. and Doyle, M. W.: Sediment–Water Surface Area Along Rivers: Water Column Versus
497 Benthic, *Ecosystems*, 21, 1505–1520, <https://doi.org/10.1007/s10021-018-0236-2>, 2018.

498 Griffiths, N. A. and Tiegs, S. D.: Organic-matter decomposition along a temperature gradient in a
499 forested headwater stream, *Freshwater Science*, 35, 518–533, 2016.

500 Grimm, N. B. and Fisher, S. G.: Stability of Periphyton and Macroinvertebrates to Disturbance by Flash
501 Floods in a Desert Stream, *Journal of the North American Benthological Society*, 8, 293–307,
502 <https://doi.org/10.2307/1467493>, 1989.

503 Hall, R. O. and Hotchkiss, E. R.: Chapter 34 - Stream Metabolism, in: *Methods in Stream Ecology* (Third
504 Edition), edited by: Lamberti, G. A. and Hauer, F. R., Academic Press, 219–233,
505 <https://doi.org/10.1016/B978-0-12-813047-6.00012-7>, 2017a.

506 Hall, R. O. and Hotchkiss, E. R.: Stream Metabolism, in: *Methods in Stream Ecology*, Academic Press,
507 219–233, <https://doi.org/10.1016/B978-0-12-813047-6.00012-7>, 2017b.

508 Hall, R. O. and Tank, J. L.: Correcting whole-stream estimates of metabolism for groundwater input,
509 *Limnology and Oceanography: Methods*, 3, 222–229, <https://doi.org/10.4319/lom.2005.3.222>, 2005.

510 Krause, S., Hannah, D. M., Fleckenstein, J. H., Heppell, C. M., Kaeser, D., Pickup, R., Pinay, G., Robertson,
511 A. L., and Wood, P. J.: Inter-disciplinary perspectives on processes in the hyporheic zone, *Ecohydrology*,
512 4, 481–499, <https://doi.org/10.1002/eco.176>, 2011.

513 Laan, M. M., Fulton, S. G., Garayburu-Caruso, V. A., Barnes, M. E., Borton, M. A., Chen, X., Farris, Y.,
514 Forbes, B., Goldman, A. E., Grieger, S., Hall Jr., R. O., Kaufman, M. H., Lin, X., Zionce, E. L. M., McKeever, S.
515 A., Myers-Pigg, A., Otenburg, O., Pelly, A. C., Ren, H., Renteria, L., Scheibe, T. D., Son, K., Tagestad, J.,
516 Torgeson, J. M., and Stegen, J. C.: Water column respiration in the Yakima River basin is explained by
517 temperature, nutrients, and suspended solids, *Biogeosciences*, 22, 6137–6152,
518 <https://doi.org/10.5194/bg-22-6137-2025>, 2025.

519 Lewandowski, J., Arnon, S., Banks, E., Batelaan, O., Betterle, A., Broecker, T., Coll, C., Drummond, J. D.,
520 Gaona Garcia, J., Galloway, J., Gomez-Velez, J., Grabowski, R. C., Herzog, S. P., Hinkelmann, R., Höhne,

521 A., Hollender, J., Horn, M. A., Jaeger, A., Krause, S., Löchner Prats, A., Magliozzi, C., Meinikmann, K.,
522 Mojarrad, B. B., Mueller, B. M., Peralta-Maraver, I., Popp, A. L., Posselt, M., Putschew, A., Radke, M.,
523 Raza, M., Riml, J., Robertson, A., Rutere, C., Schaper, J. L., Schirmer, M., Schulz, H., Shanafield, M., Singh,
524 T., Ward, A. S., Wolke, P., Wörman, A., and Wu, L.: Is the Hyporheic Zone Relevant beyond the Scientific
525 Community?, *Water*, 11, 2230, <https://doi.org/10.3390/w11112230>, 2019.

526 Mancuso, J., Messick, E., and Tiegs, S. D.: Parsing spatial and temporal variation in stream ecosystem
527 functioning, *Ecosphere*, 13, e4202, <https://doi.org/10.1002/ecs2.4202>, 2022.

528 Mancuso, J., Tank, J. L., Mahl, U. H., Vincent, A., and Tiegs, S. D.: Monthly variation in organic-matter
529 decomposition in agricultural stream and riparian ecosystems, *Aquat Sci*, 85, 83,
530 <https://doi.org/10.1007/s00027-023-00975-7>, 2023.

531 McClain, M. E., Boyer, E. W., Dent, C. L., Gergel, S. E., Grimm, N. B., Groffman, P. M., Hart, S. C., Harvey,
532 J. W., Johnston, C. A., Mayorga, E., McDowell, W. H., and Pinay, G.: Biogeochemical Hot Spots and Hot
533 Moments at the Interface of Terrestrial and Aquatic Ecosystems, *Ecosystems*, 6, 301–312, 2003.

534 Mulholland, P. J., Fellows, C. S., Tank, J. L., Grimm, N. B., Webster, J. R., Hamilton, S. K., Martí, E.,
535 Ashkenas, L., Bowden, W. B., Dodds, W. K., McDowell, W. H., Paul, M. J., and Peterson, B. J.: Inter-biome
536 comparison of factors controlling stream metabolism, *Freshwater Biology*, 46, 1503–1517,
537 <https://doi.org/10.1046/j.1365-2427.2001.00773.x>, 2001.

538 Naegeli, M. W. and Uehlinger, U.: Contribution of the hyporheic zone to ecosystem metabolism in a
539 prealpine gravel-bed-river, *Journal of the North American Benthological Society*, 16, 794–804, 1997.

540 Odum, H. T.: Primary production in flowing waters 1, *Limnology and oceanography*, 1, 102–117, 1956.

541 Piatka, D. R., Wild, R., Hartmann, J., Kaule, R., Kaule, L., Gilfedder, B., Peiffer, S., Geist, J., Beierkuhnlein,
542 C., and Barth, J. A. C.: Transfer and transformations of oxygen in rivers as catchment reflectors of
543 continental landscapes: A review, *Earth-Science Reviews*, 220, 103729,
544 <https://doi.org/10.1016/j.earscirev.2021.103729>, 2021.

545 Pingram, M. A., Clapcott, J. E., Hamer, M. P., Atalah, J., and Özkundakci, D.: Exploring temporal and
546 spatial variation in cotton tensile-strength loss to assess the ecosystem health of non-wadeable rivers,
547 *Ecological Indicators*, 108, 105773, <https://doi.org/10.1016/j.ecolind.2019.105773>, 2020.

548 Roley, S. S., Hall Jr., R. O., Perkins, W., Garayburu-Caruso, V. A., and Stegen, J. C.: Coupled primary
549 production and respiration in a large river contrasts with smaller rivers and streams, *Limnology and
550 Oceanography*, 68, 2461–2475, <https://doi.org/10.1002/lno.12435>, 2023.

551 Talluto, L., del Campo, R., Estévez, E., Altermatt, F., Datry, T., and Singer, G.: Towards (better) fluvial
552 meta-ecosystem ecology: a research perspective, *npj biodiversity*, 3, 1–10,
553 <https://doi.org/10.1038/s44185-023-00036-0>, 2024.

554 Tank, J. L., Rosi-Marshall, E. J., Griffiths, N. A., Entekin, S. A., and Stephen, M. L.: A review of
555 allochthonous organic matter dynamics and metabolism in streams, *Journal of the North American
556 Benthological Society*, 29, 118–146, 2010.

557 Tiegs, S. D., Clapcott, J. E., Griffiths, N. A., and Boulton, A. J.: A standardized cotton-strip assay for
558 measuring organic-matter decomposition in streams, *Ecological Indicators*, 32, 131–139,
559 <https://doi.org/10.1016/j.ecolind.2013.03.013>, 2013.

560 Tiegs, S. D., Costello, D. M., Isken, M. W., Woodward, G., McIntyre, P. B., Gessner, M. O., Chauvet, E.,
561 Griffiths, N. A., Flecker, A. S., Acuña, V., Albariño, R., Allen, D. C., Alonso, C., Andino, P., Arango, C.,
562 Aroviita, J., Barbosa, M. V. M., Barmuta, L. A., Baxter, C. V., Bell, T. D. C., Bellinger, B., Boyero, L., Brown,
563 L. E., Bruder, A., Bruesewitz, D. A., Burdon, F. J., Callisto, M., Canhoto, C., Capps, K. A., Castillo, M. M.,
564 Clapcott, J., Colas, F., Colón-Gaud, C., Cornut, J., Crespo-Pérez, V., Cross, W. F., Culp, J. M., Danger, M.,
565 Dangles, O., Eyto, E. de, Derry, A. M., Villanueva, V. D., Douglas, M. M., Elosegí, A., Encalada, A. C.,
566 Entekin, S., Espinosa, R., Ethaiya, D., Ferreira, V., Ferriol, C., Flanagan, K. M., Fleituch, T., Shah, J. J. F.,
567 Frainer, A., Friberg, N., Frost, P. C., Garcia, E. A., Lago, L. G., Soto, P. E. G., Ghate, S., Giling, D. P., Gilmer,
568 A., Gonçalves, J. F., Gonzales, R. K., Graça, M. A. S., Grace, M., Grossart, H.-P., Guérol, F., Gulis, V.,
569 Hepp, L. U., Higgins, S., Hishi, T., Huddart, J., Hudson, J., Imberger, S., Iñiguez-Armijos, C., Iwata, T.,
570 Janetski, D. J., Jennings, E., Kirkwood, A. E., Koning, A. A., Kosten, S., Kuehn, K. A., Laudon, H., Leavitt, P.
571 R., Silva, A. L. L. da, Leroux, S. J., LeRoy, C. J., Lisi, P. J., MacKenzie, R., Marcarelli, A. M., Masese, F. O.,
572 McKie, B. G., Medeiros, A. O., Meissner, K., Miliša, M., Mishra, S., Miyake, Y., Moerke, A., et al.: Global
573 patterns and drivers of ecosystem functioning in rivers and riparian zones, *Science Advances*, 5,
574 eaav0486, <https://doi.org/10.1126/sciadv.aav0486>, 2019.

575 Tiegs, S. D., Capps, K. A., Costello, D. M., Schmidt, J. P., Patrick, C. J., Follstad Shah, J. J., Leroy, C. J., and
576 CELLDEX Consortium†: Human activities shape global patterns of decomposition rates in rivers, *Science*,
577 384, 1191–1195, 2024.

578 Vyšná, V., Dyer, F., Maher, W., and Norris, R.: Cotton-strip decomposition rate as a river condition
579 indicator – Diel temperature range and deployment season and length also matter, *Ecological Indicators*,
580 45, 508–521, <https://doi.org/10.1016/j.ecolind.2014.05.011>, 2014.

581 Webb, J. R., Pearce, N. J. T., Painter, K. J., and Yates, A. G.: Hierarchical variation in cellulose
582 decomposition in least-disturbed reference streams: a multi-season study using the cotton strip assay,
583 *Landscape Ecol*, 34, 2353–2369, <https://doi.org/10.1007/s10980-019-00893-w>, 2019.

584 Wondzell, S. M.: The role of the hyporheic zone across stream networks, *Hydrological Processes*, 25,
585 3525–3532, <https://doi.org/10.1002/hyp.8119>, 2011.

586 Woodward, G., Gessner, M. O., Giller, P. S., Gulis, V., Hladyz, S., Lecerf, A., Malmqvist, B., McKie, B. G.,
587 Tiegs, S. D., and Cariss, H.: Continental-scale effects of nutrient pollution on stream ecosystem
588 functioning, *Science*, 336, 1438–1440, 2012.

589 Young, R. G. and Collier, K. J.: Contrasting responses to catchment modification among a range of
590 functional and structural indicators of river ecosystem health, *Freshwater Biology*, 54, 2155–2170,
591 <https://doi.org/10.1111/j.1365-2427.2009.02239.x>, 2009.

592 Young, R. G. and Huryn, A. D.: Effects of Land Use on Stream Metabolism and Organic Matter Turnover,
593 *Ecological Applications*, 9, 1359–1376, [https://doi.org/10.1890/1051-
594 0761\(1999\)009%255B1359:EOLUOS%25D2.0.CO;2](https://doi.org/10.1890/1051-0761(1999)009%255B1359:EOLUOS%25D2.0.CO;2), 1999.

595 Zarnetske, J. P., Haggerty, R., Wondzell, S. M., and Baker, M. A.: Dynamics of nitrate production and
596 removal as a function of residence time in the hyporheic zone, *Journal of Geophysical Research:*
597 *Biogeosciences*, 116, <https://doi.org/10.1029/2010JG001356>, 2011.

598

599

600

601

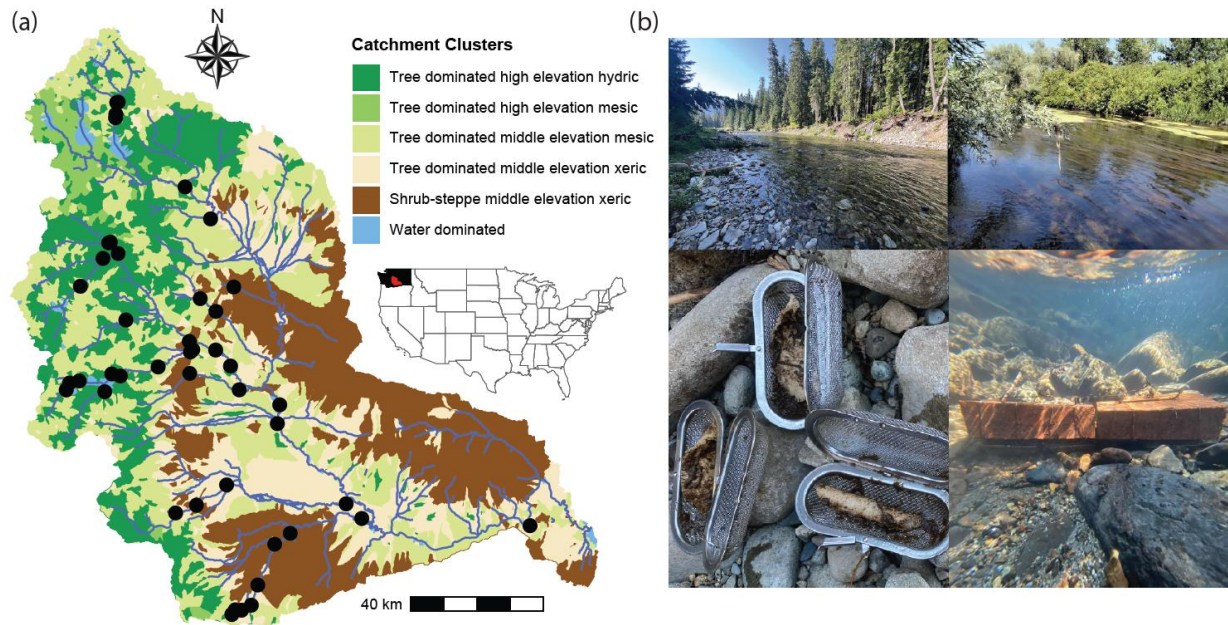
602

603

604

605

606 **Figures**

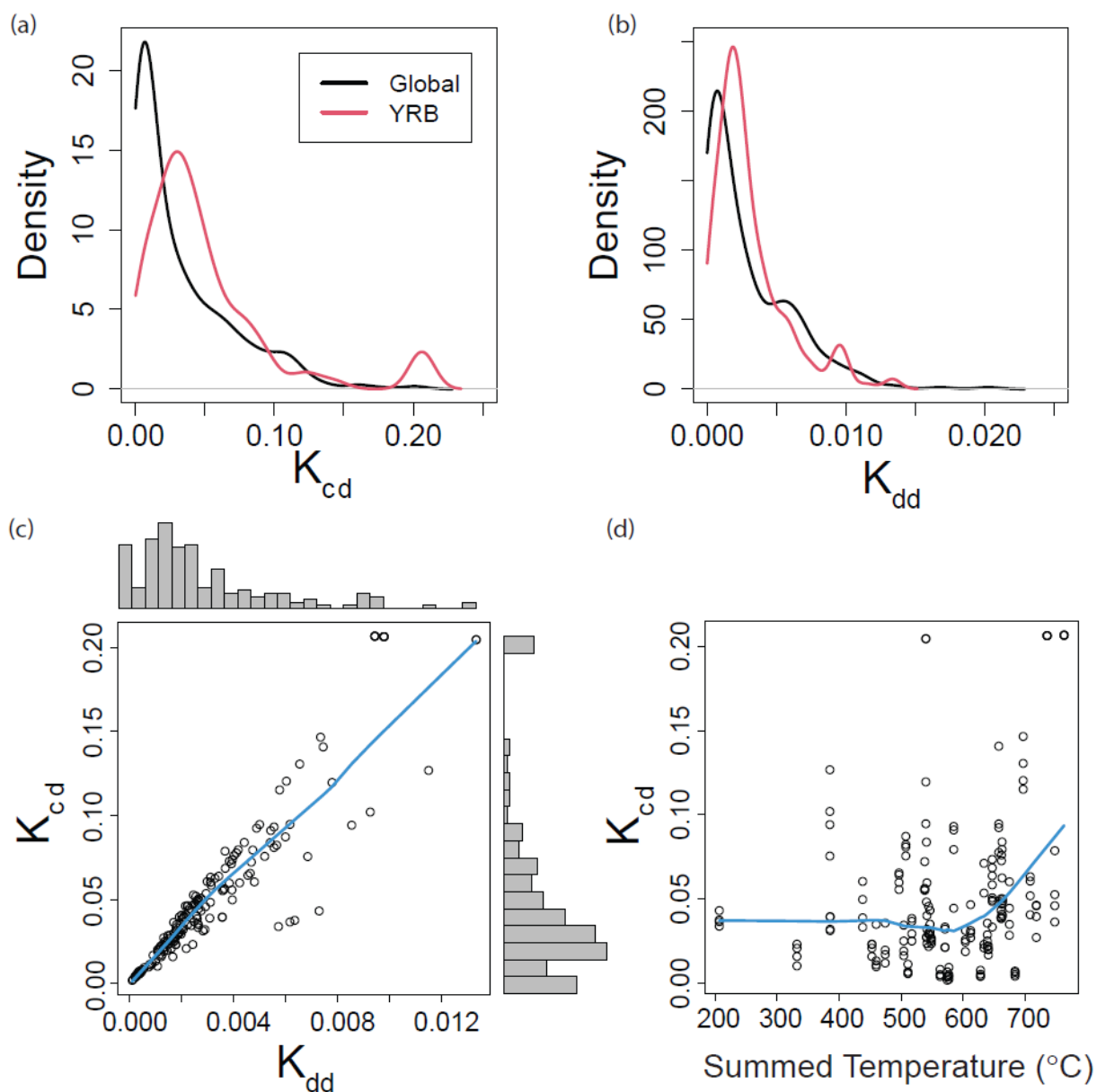


607

608 **Figure 1. Biophysical clusters, sampling locations, and example conditions across the YRB.** (a) The inset
609 map shows the location of the YRB within the contiguous United States, with black indicating
610 Washington State and red indicating the YRB. The YRB is shown with multiple colors, which correspond
611 to biophysical clusters, as presented in Laan et al. (2025) and summarized briefly in the legend. Black
612 circles are locations where decay rates were estimated. (b) Photos provide examples of the breadth of
613 conditions studied across the YRB, post-incubation states of cotton strips, and deployment of the cotton
614 strips.

615

616

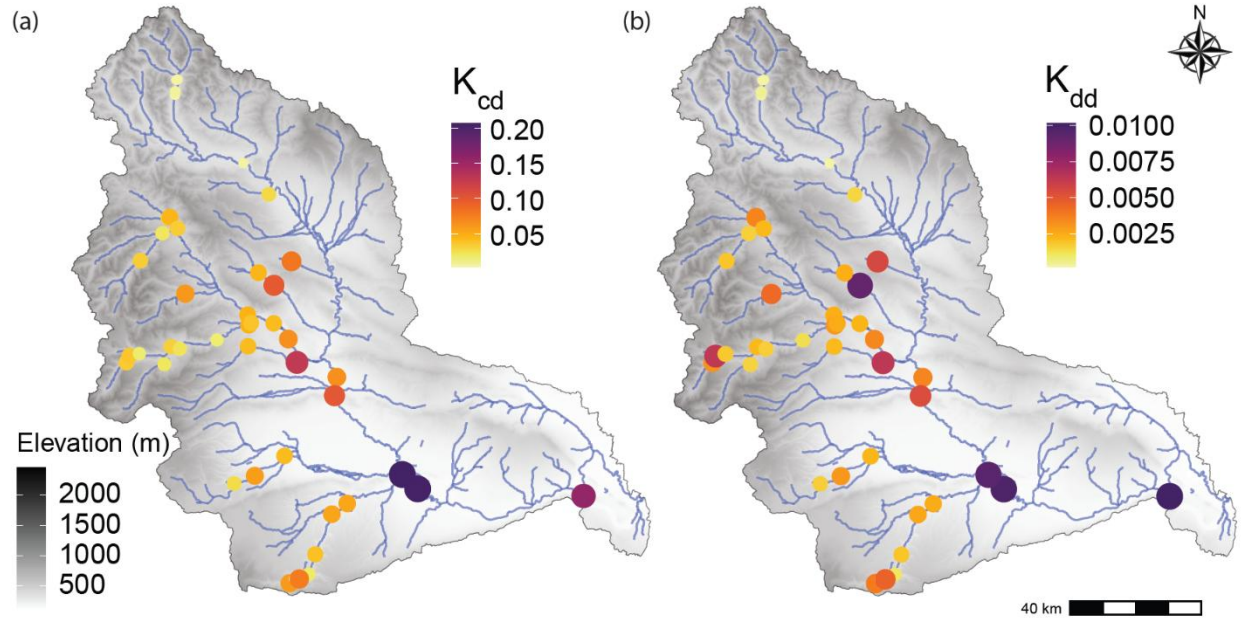


617

618 **Figure 2. Decay rate distributions and relationships to each other and temperature.** Kernel density
619 functions for (a) K_{cd} and (b) K_{dd} from a global streams and rivers dataset and from the YRB. (c)
620 Scatterplot correlating K_{cd} to K_{dd} . Histograms summarizing the distribution of each rate are provided on
621 the outer boundaries. (d) K_{cd} related to temperature summed across the deployment period; summed
622 temperature was used to calculate K_{dd} . Blue lines represent Lowess spline fits as regression analysis was
623 not required for interpretation.

624

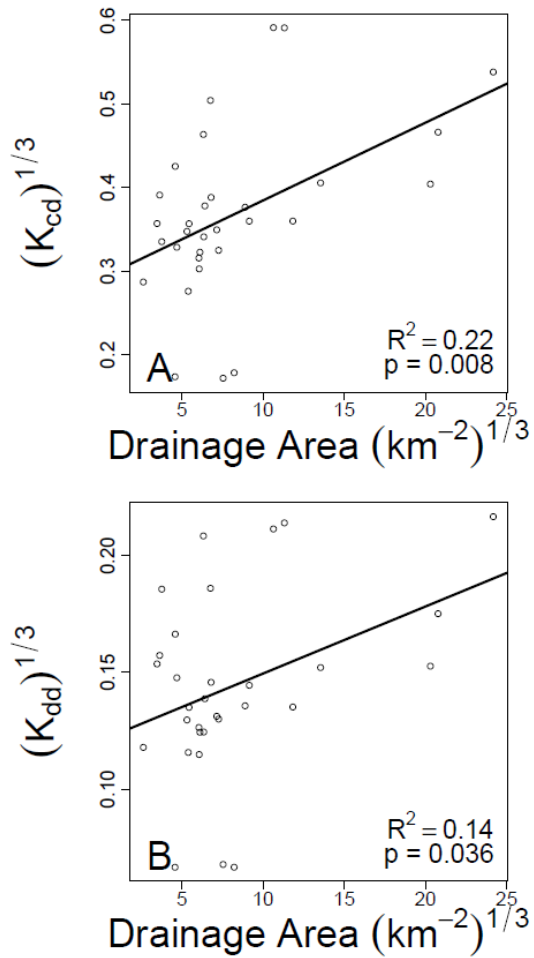
625



626

627 **Figure 3: Spatial distribution of decay rates across the YRB.** Each map shows elevation profiles and
 628 either K_{cd} (A) or K_{dd} (B). Colored circles are field locations where rates were estimated. The color of each
 629 circle is related to decay rate as indicated in the legends, and circle size is scaled to decay rate to further
 630 facilitate visual interpretability.

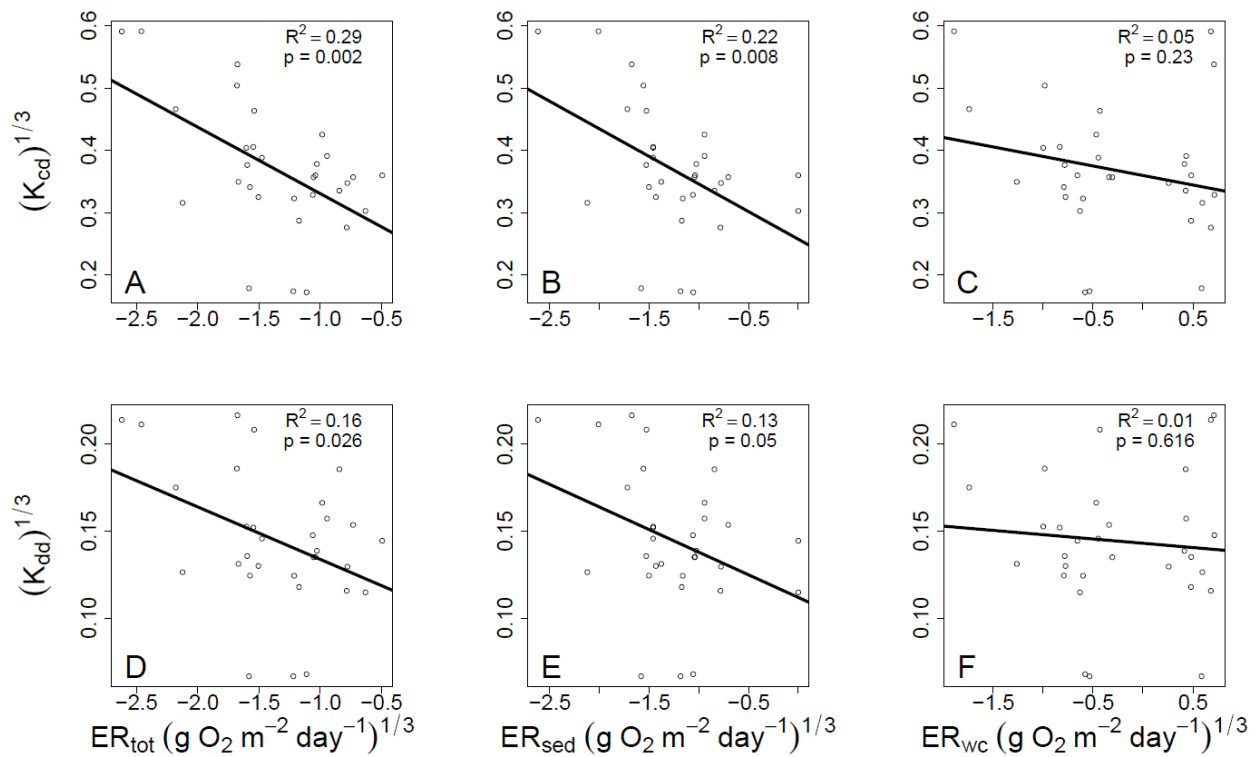
631



632

633 **Figure 4. Decay rates increase with drainage area.** K_{cd} (A) and K_{dd} (B) regressed against upstream
 634 drainage area and fit with an ordinary least squares linear regression. Associated regression models are
 635 shown as solid black lines and statistics are provided on each panel. Data were cube root transformed to
 636 improve normality before analysis.

637



639

640 **Figure 5: Decay rates related to each of the three aspects of stream ecosystem respiration.** Both K_{cd} (A-
 641 C) and K_{dd} (D-F) show strongest relationships with ER_{tot} (A,D), weaker relationships with ER_{sed} (B,E), and
 642 non-significant relationships with ER_{wc} (C,F). Ordinary least squares linear regression models are shown
 643 and with solid black lines and associated statistics are provided on each panel. All variables were cube-
 644 root transformed to improve normality prior to regression analysis.

645

646 **Tables**

647 **Table 1.** Comparison of univariate and multivariate regression models explaining variation in K_{cd} and K_{dd} .
 648 Model structures are indicated, along with change in AIC relative to the best model. ER_{tot} was not used
 649 in multivariate models because $ER_{tot} = ER_{sed} + ER_{wc}$. Regression statistics for the univariate models are
 650 provided in Figure 5; only the best performing univariate models, in terms of R^2 , are shown. The models
 651 with ER_{sed} and ER_{wc} , but not the interaction term, are effectively the same as the ER_{tot} model because
 652 $ER_{tot} = ER_{sed} + ER_{wc}$. They are included as a point of reference for the model that also includes the
 653 $ER_{sed} * ER_{wc}$ interaction term.

Model	Δ AIC
$K_{cd} \sim ER_{tot}$	0
$K_{cd} \sim ER_{sed} + ER_{wc}$	3.8
$K_{cd} \sim ER_{sed} + ER_{wc} + ER_{sed} * ER_{wc}$	5.7
$K_{dd} \sim ER_{tot}$	0
$K_{dd} \sim ER_{sed} + ER_{wc}$	3.0
$K_{dd} \sim ER_{sed} + ER_{wc} + ER_{sed} * ER_{wc}$	4.8

654

655 **Table 2.** Regression coefficients from LASSO models explaining variation in K_{dd} and K_{cd} . Explanatory
 656 variables were cube root transformed to reduce influence from high leverage data points and
 657 standardized as z-scores to enable direct comparison of the regression coefficients. LASSO models were
 658 fit over 100 seeds. Regression coefficients (β) and R^2 values were averaged across the 100 seeds.
 659 Normalized regression coefficients were calculated by dividing each β coefficient by the maximum β
 660 coefficient in each seed. Standard deviation (sd) is reported for each variables' coefficient over the 100
 661 seeds and used to calculate the coefficient of variation (cv). Variables shown have an absolute value of
 662 mean normalized β of > 0.5 and $cv < 0.5$ to emphasize variables that were consistently important across
 663 seeds. Results for all variables, both normalized and not normalized, can be found in Table S1.

Response Variable	Predictor Variable	Mean Normalized Regression Coefficient (β)	sd	cv
K_{dd}	Water TDN	1	0	0
	D50	-0.699	0.087	-0.124
Mean R^2			0.502 (sd = 0.0673)	
K_{cd}	Aridity	-0.959	0.065	-0.067
	Water TDN	0.805	0.156	0.193
Mean R^2			0.883 (sd = 0.083)	

664

665

666

667

668